Time-Resolved Two-Photon Photoemission of Unoccupied Electronic States of Periodically Rippled Graphene on Ru(0001)

N. Armbrust,[1] J. Güdde,[1] P. Jakob,[1] and U. Höfer[1,2]

[1]*Fachbereich Physik und Zentrum für Materialwissenschaften, Philipps-Universität, 35032 Marburg, Germany*

[2]*Donostia International Physics Center (DIPC), 20018 San Sebastián, Spain*

(Received 29 September 2011; published 31 January 2012)

The unoccupied electronic states of epitaxially grown graphene on Ru(0001) have been explored by time- and angle-resolved two-photon photoemission. We identify a Ru derived resonance and a Ru/graphene interface state at 0.91 and 2.58 eV above the Fermi level, as well as three image-potential derived states close to the vacuum level. The most strongly bound, short-lived, and least dispersing image-potential state is suggested to have some quantum-well character with a large amplitude below the graphene hills. The two other image-potential states are attributed to a series of slightly decoupled states. Their lifetimes and dispersions are indicative of electrons moving almost freely above the valley areas of the moiré superstructure of graphene.

DOI: 10.1103/PhysRevLett.108.056801 PACS numbers: 73.20.−r, 73.22.Pr, 78.47.J−, 79.60.Dp

There is fast-growing interest in understanding the interaction of graphene with metal substrates. By means of thermal decomposition of unsaturated hydrocarbon species on transition metal substrates, the fabrication of very large and extremely well-defined graphene sheets can be realized [1,2]. Moreover, metal contacts are of high relevance to graphene-based electronic devices. In terms of the electronic structure, angle-resolved photoelectron spectroscopy has already provided information about the occupied states of graphene on different substrates [3,4]. Comparatively little, however, is known about unoccupied states above the Fermi level and even less on dynamics of electron transfer processes between graphene layers and metals. In addition to spectroscopic features originating from surface states of the metal and/or π bands of graphene, the normally unoccupied image-potential states [5] are expected to depend sensitively on the graphene-metal interaction. Previous two-photon photoemission (2PPE) studies have shown that thin dielectric overlayers strongly modify these metal-derived states [6–8]. Graphene, due to its high in-plane polarizability, gives rise to its own series of image-potential states [9,10]. It is an interesting open question to which extent this affects the properties of the graphene-metal system.

In this Letter, we use time-resolved 2PPE to determine energies, lifetimes, and dispersions of unoccupied states in the full energy range between the Fermi and the vacuum level of single graphene layers on Ru(0001). Graphene/Ru(0001) [g/Ru(0001)] is an interesting case because of a relatively strong geometrical corrugation of the graphene sheets [11,12]. The C-Ru distance varies between 2.2 Å in the strongly interacting L areas (valleys) of the hexagonal moiré superlattice and 3.7 Å in the H areas (hills) [12–14]. Using scanning-tunnelling spectroscopy (STS) a series of field-emission resonances, i.e., Stark shifted image-potential states, have been observed [15,16]. However, the detailed assignment of these resonances and the interpretation of other states located at the hill and valley areas are discussed controversially [15–18].

Our 2PPE spectra of g/Ru(0001) show five dispersing unoccupied states between the Fermi level E_F and the vacuum level E_{vac} with lifetimes ranging from 10 up to 85 fs. The properties of three of these states clearly identify them as image-potential-derived states near the vacuum level, 3.5–4.0 eV above the Fermi level. Their perpendicular coupling to the Ru substrate as well as their lateral mobility are seen to be strongly affected by the corrugated graphene layer. The other two states are observed at energies of 0.91 and 2.58 eV above the Fermi level, and exhibit a larger overlap with the bulk metal than the higher lying states. Most likely, they originate from the well-known surface resonance of clean Ru(0001), subject to distinct energy shifts, depending on the graphene-Ru distances in the H and L regions [15].

The experiments have been conducted under ultrahigh vacuum conditions using a 2PPE setup described previously [19]. The photon energies of the p-polarized blue and ultraviolet (uv) laser pulses were 3.10 and 4.70 eV with pulse lengths of 50 and 65 fs, respectively. This two-color setup allows us to access the complete energy range between E_F and E_{vac}. The overall energy resolution was 70 meV, the angular resolution 2°. The angle between the laser beam and the detection of the photoelectrons was 75°. Well-defined graphene monolayers on Ru(0001) have been prepared by decomposition of ethylene at elevated temperatures, as described in Ref. [20]. The graphene layer reduces the work function of Ru ($\Phi_{\mathrm{Ru}} = 5.51 \pm 0.05$ eV) to $\Phi = 4.24 \pm 0.10$ eV as derived from the 2PPE spectra. This value conforms with the higher local work function of the H areas given in Ref. [21] as compared to the 0.24 eV lower value of the L areas. The sample temperature was $T \approx 80$ K throughout all measurements.

2PPE spectra of g/Ru(0001) show a number of peaks and structures [Fig. 1(a)]. Depending on the energy of the photoemitting probe pulse, features observed at a certain kinetic energy originate from different intermediate-state energies. The assignment is possible by comparing the two-color uv + blue with single-color 2PPE spectra. Note that both the uv and the blue laser pulses can play the role of excitation and probe pulses [Fig. 1(b)].

In the uv + blue two-color spectra prominent features denoted $n = 1'$, $n = 1$, and $n = 2$ are observed in the range 6.5–7.0 eV. In the uv single-color (and with virtually identical trace in the uv + blue two-color spectra) they appear at final-state energies between 8.0 and 8.5 eV. In the blue spectrum, on the other hand, they are entirely missing. Obviously, population of these states requires uv photons, whereas photoemission can be accomplished by blue as well as by uv photons. The intermediate-state energies of these features (3.44, 3.59, 3.82 eV) are slightly below E_{vac}. In accordance with measurements taken with variable time delay between the uv pump and the blue probe pulses (see below), they are identified as image-potential states.

The prominent peak S in the uv + blue spectra at 7.23 eV is visible at the same final-state energy in the uv, but not in the blue spectrum. This suggests that it is probed by uv photons. The corresponding intermediate-state energy is thus 2.58 eV, i.e., much smaller than that of the states $n = 1'$, 1, and 2 which appear below peak S when probed by blue laser pulses, i.e., with 1.60 eV lower photon energy. Electrons from intermediate-state S at 2.58 eV can also be photoemitted by blue photons and a corresponding peak appears at the lower part of the spectra at 5.6-eV final-state energy. Note, however, that the weak feature visible in the uv spectrum at about similar energies has a different origin. It corresponds to another intermediate state, labeled S' and located 0.91 eV above E_F. In this energy range an unoccupied state has been observed with inverse photoemission for clean Ru [22]. This suggests that S' is derived from the Ru surface resonance, subject to a mild energetic shift, as expected for the H areas of g/Ru(0001). The fact that the 5.6-eV peak of the uv + blue spectrum contains contributions of the state S', in addition to S, will be exploited in the time-resolved experiments discussed below.

The assignments above are corroborated by measurements as a function of the probe pulse photon energy (see Supplemental Material [23]). The additional peak labeled d at $E - E_F = 6.1$ eV can be assigned to transitions from the uppermost occupied d band of Ru just below E_F [24].

The energy positions of the states $n = 1', 1, 2$ and S deduced from 2PPE spectra taken at different emission angles are displayed in Fig. 2 as a function of parallel momentum $k_{\parallel} = \sqrt{2mE_{kin}/\hbar^2}\sin(\theta)$. These measurements were performed by varying the angle θ between the sample normal and the direction of electron detection. Specifically, we probed at an orientation 7° off from the $\bar{\Gamma}$-$\bar{K}$ direction [Fig. 2(c)]. All states show an upward dispersion at the $\bar{\Gamma}$ point and backfolding at the Brillouin zone boundary of the (12.5×12.5) subunit of the moiré superstructure at $k_{\parallel,moiré} = 0.135$ Å^{-1} (dashed line) [25]. The behavior at the zone boundary underscores the intimate relation of these states with the g/Ru(0001) moiré superstructure.

Lifetimes of electrons excited into the various states have been determined at the $\bar{\Gamma}$ point either by delaying the blue pulses with respect to the uv pulses [states $n = 1', 1, 2$ in Fig. 3(a)] or vice versa [states S, S' in Fig. 3(b)]. The states $n = 1', 1$ as well as S and S' exhibit very short

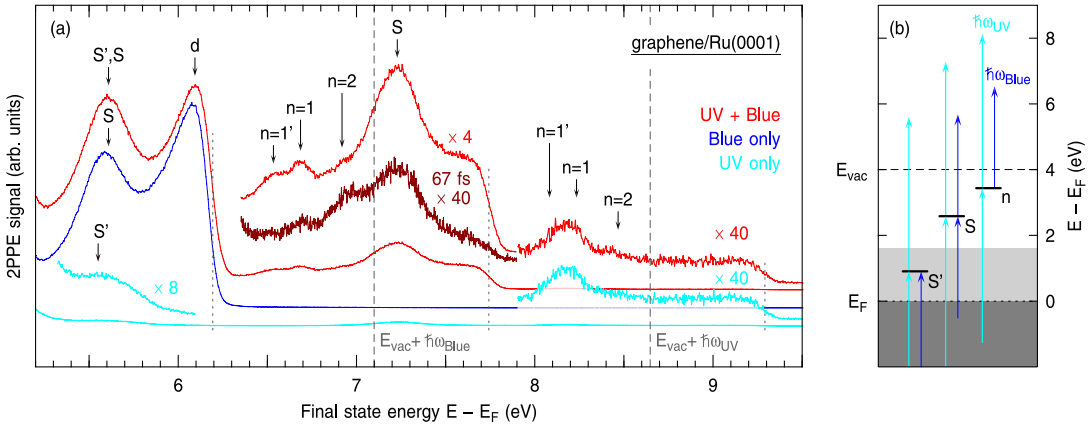

FIG. 1 (color online). (a) 2PPE spectra of g/Ru(0001) in normal emission for different combinations of blue and uv laser pulses. The lower (cyan) [middle (blue)] curve shows single-color uv (blue) spectra. For the upper (red) spectra, both laser pulses were incident. The time delay between uv and blue pulses was 0 (not indicated) or 67 fs. Dotted lines indicate the final-state energies $E_F + 2 \times \hbar\omega_{blue}$, $E_F + \hbar\omega_{blue} + \hbar\omega_{uv}$, and $E_F + 2 \times \hbar\omega_{uv}$ of electrons photoemitted from the Fermi level E_F by direct two-photon photoemission. Dashed lines indicate the position of vacuum level E_{vac} of the L areas for photoemission with blue and uv pulses, respectively. (b) Excitation scheme for the different combinations of blue (short arrows) and uv (long arrows) laser pulses. Dark gray and light gray areas illustrate the occupied and unoccupied states of the valence band, respectively.

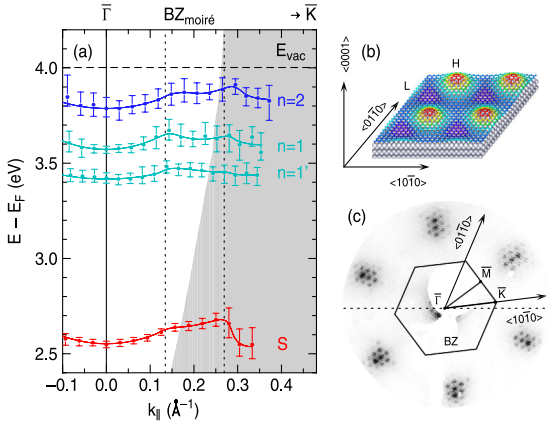

FIG. 2 (color online). (a) Dispersion of the surface and image-potential states. Solid lines are a guide to the eye. The zone boundary of the (12.5 × 12.5) subunit of the g/Ru(0001) supercell ($BZ_{moiré}$) is illustrated as vertical dashed line. Shaded gray areas depict the projected bulk band structure of Ru(0001) [30]. E_{vac} denotes the vacuum level in the L areas. (b) Sketch of g/Ru(0001) in real space. (c) LEED picture with the surface Brillouin zone (BZ) of Ru(0001). The dispersion has been measured along the horizontal dotted line.

lifetimes in the range of 20 fs and below. Since the cross correlation of the two laser pulses is the same for all pump-probe traces, the trends of the measured lifetimes are very reliable, despite an overall error margin of their absolute values of ≥ 5 fs. The weak feature $n = 2$ is located in the wing of peak S [Fig. 1(a)]. Consequently, the decay of the 2PPE intensity at this energy consists of two components. The intense but fast decaying component results from pumping state S with blue light and probing with uv; the less intense, more slowly decaying component arises from the population of $n = 2$ with uv light and probing with blue. The lifetime of the $n = 2$ component is 85 fs.

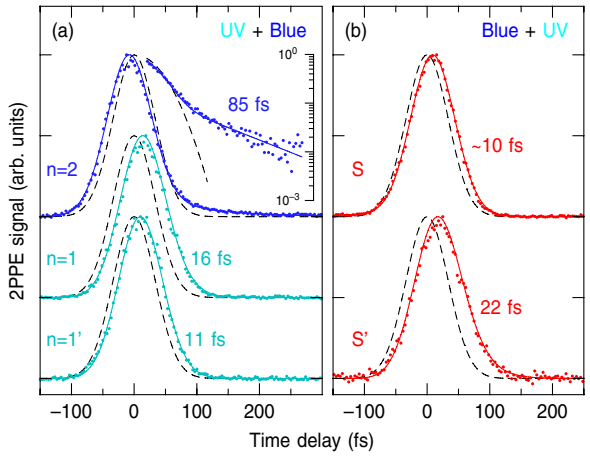

FIG. 3 (color online). 2PPE intensity at the peak maxima of states $n = 1', 1, 2$, S and S' as a function of time delay between uv pump and blue probe pulses (a) and vice versa (b). Dots show experimental data, solid lines depict best fits using a rate-equation model for the population decay with lifetimes as indicated, dashed lines denote the cross correlation between pump and probe pulses. For $n = 2$ the data are additionally displayed in a logarithmic vertical scale.

The energies of the states, their effective masses (determined for $-0.06 \leq k_{\parallel} \leq 0.12$ Å^{-1}), and lifetimes at the $\bar{\Gamma}$ point are collected in Table I. Based on these results, a consistent picture of the unoccupied electronic states at the g/Ru(0001) surface can be developed. In the following we will relate the lifetimes of the states to their localization perpendicular to the Ru surface. To a first approximation the decay rate, i.e., the inverse lifetime, is proportional to the wave function overlap of the excited electrons with the Ru substrate and to the phase space for electron-hole-pair creation [26]. The latter increases with the energy above E_F. Because of a high density of d states near E_F in Ru, it is very unlikely that electronic excitations in the graphene layer will play an important role for the decay.

State S is energetically close to the 3-eV peak observed by STS in L areas of g/Ru(0001) [15,16]. Whereas Zhang *et al.* [16,17] assigned this peak to the first member of the series of field-emission resonances in the L areas, Borca *et al.* proposed that the strong interaction of graphene with Ru in the L areas results in a substantial up-shift of the Ru(0001) surface resonance [15,18]. The energy of state S located 1.4 eV below E_{vac} clearly excludes an assignment as an image-potential state and thus field-emission resonance. Furthermore, the lifetime of state S is quite short and similar to $n = 1'$, although S is much closer to E_F. This indicates a significantly larger overlap of state S with the metal than that of the image-potential states. Both results are consistent with its interpretation as an up-shifted surface resonance by Borca *et al.* [15].

According to its energy of 0.91 eV above E_F, state S' may be identified as the same surface state in the H areas; due to the larger graphene to Ru distance, such a state is subject to a much weaker up-shift as compared to the L areas. Its longer lifetime correlates well with its smaller energy with respect to E_F. The increase of the lifetime of S' compared to S, however, is smaller than expected from this argument. This indicates that S' has a larger overlap with the metal than S, and little or no overlap with graphene. The character of S' is therefore closer to the intrinsic Ru(0001) surface resonance. It also explains the fact that S' is not observed by STS. This state is almost completely

TABLE I. Energies $E - E_F$, lifetimes τ, effective masses m_{eff}, and location within the g/Ru(0001) unit cell of image-potential states $n = 1', 1, 2$ and surface states S and S' of g/Ru(0001).

State	$E - E_F$ (eV)	τ (fs)	m_{eff}	Area
$n = 2$	3.82 ± 0.07	85 ± 13	1.2 ± 0.6	
$n = 1$	3.59 ± 0.05	16 ± 5	0.8 ± 0.3	L
$n = 1'$	3.44 ± 0.05	11 ± 8	2.1 ± 0.8	H
S	2.58 ± 0.04	10 ± 12	1.0 ± 0.2	L
S'	0.91 ± 0.06	22 ± 5		H

buried underneath the graphene layer in the H areas and has a vanishing overlap with the STM tip.

Since the natural reference level of image-potential states is the vacuum level, it is tempting to relate the ($n = 1'$) state at lower energies to the L areas with their lower local work function of $\Phi = 4.0$ eV, and $n = 1$ at higher energy to a state at the H areas where $\Phi = 4.24$ eV. Both states would then exhibit similar binding energies with respect to the local vacuum level ($E_{1'} = 0.56$ eV, $E_1 = 0.65$ eV). However, the longer lifetime of the ($n = 1$) state and its smaller effective mass are difficult to reconcile with this interpretation. Instead, a consistent picture is obtained from a reversed assignment: With respect to the local work function of the H areas ($\Phi = 4.24$ eV), state $n = 1'$ has a binding energy of 0.8 eV. This is slightly higher compared to 0.65 eV on clean Ru(0001) [27,28]. The energy of state $n = 1$ with respect to the local work function of the L areas ($\Phi = 4.0$ eV) is then 0.41 eV. This matches perfectly with the shorter lifetime of $n = 1'$. In general, more strongly bound image-potential states are localized closer to the substrate, leading to a faster decay.

Quantitatively, the value of 11 fs for $n = 1'$ is similar to the lifetime of the first image-potential state on clean Ru(0001) [27,28]. Because of the high density of Ru d states in the vicinity of E_F these decay times are considerably shorter than in the case of Cu(100) with a similar band gap. The significantly longer lifetime and lower binding energy of $n = 1$ as compared to $n = 1'$ then suggests that image-potential electrons have less overlap with the metal in the L areas than in the H areas. This is surprising only at first glance, since a graphene overlayer in close contact with the metal will have a tendency to push the wave function of the image-potential states away from the metal surface. As the distance becomes larger, the Ru surface and the graphene layer can act as a quantum well and the wave function develops a local maximum in between the metal surface and graphene. On an ideal metal surface the maximum of the ($n = 1$) wave function is located about 2 Å away from the image plane [5]. With a Ru-C distance of 3.7 Å the H areas can therefore accommodate a considerable amount of the ($n = 1'$) wave function below the graphene layer. For similar reasons the binding energies and lifetimes of image-potential states of some rare-gas overlayers on metal surfaces show oscillations as a function of layer thickness [6,8]. We also note that, based on a similar argument, it has been proposed that interlayer states of graphite result from trapping of the most strongly bound image-potential state of a single sheet of graphene [9]. The assignment is consistent with the higher effective mass of the ($n = 1'$) state because the motion of the image-state electron, partially located below the hill areas, is hindered as the graphene layer bends down towards the valley regions.

The observation of a single ($n = 2$) state is consistent for the following reason: the height modulation of the graphene layer by 1.5 Å represents only a slight distortion for a ($n = 2$) wave function whose maximum is about 11 Å away from the image plane of a metal surface [5]. The ($n = 2$) wave function will therefore be fully delocalized over the g/Ru(0001) moiré structure in accordance with the observed nearly free-electron-like dispersion. Nevertheless, this state will, like the ($n = 1$) state, have a higher probability density in the L areas where the local work function is lower. This is in agreement with the observation of a lower amplitude of the field-emission resonances in the H areas as probed by STS [15]. With respect to the work function in the L areas, the ($n = 2$) binding energy amounts to 0.18 eV, which fits well to a ($n = 2$) state that is slightly decoupled from the Ru surface. This decoupling is also reflected in its lifetime of 85 fs which is longer than on the clean Ru(0001) where 55 fs has been reported [28].

In conclusion, we have shown that the periodic moiré superstructure of epitaxially grown graphene on Ru(0001) exhibits a number of novelties referring to image-potential and surface or interface states. On the one hand, a series of slightly decoupled image-potential states $n = 1, 2, \ldots$ have been observed and associated with almost free-moving electrons, predominantly located in the valley areas. On the other hand, an additional image-potential state $n = 1'$ has been identified whose wave function has a substantial amplitude below the graphene hills. This results in a larger binding energy, a shorter lifetime, and a higher effective mass of this state. Note that such a splitting of the first image-potential state is not observed for g/Ir(111) which is more weakly interacting and does not show the strong corrugation of g/Ru(0001) [29]. Finally, the dissimilar graphene-Ru distances in the L and H areas lead to different confinement and energy shifts of the Ru(0001) surface resonance. This explains the appearance of two additional unoccupied states S and S'.

We thank A. Arnau, P. M. Echenique, and D. Sánchez-Portal for valuable discussions and gratefully acknowledge funding by the Deutsche Forschungsgemeinschaft through GK 790 and the Ikerbasque foundation.

[1] T. A. Land, T. Michely, R. J. Behm, J. C. Hemminger, and G. Comsa, Surf. Sci. **264**, 261 (1992).
[2] S. Marchini, S. Günther, and J. Wintterlin, Phys. Rev. B **76**, 075429 (2007).
[3] P. Sutter, M. S. Hybertsen, J. T. Sadowski, and E. Sutter, Nano Lett. **9**, 2654 (2009).
[4] I. Pletikosić, M. Kralj, P. Pervan, R. Brako, J. Coraux, A. T. N'Diaye, C. Busse, and T. Michely, Phys. Rev. Lett. **102**, 056808 (2009).
[5] P. M. Echenique and J. B. Pendry, J. Phys. C **11**, 2065 (1978).
[6] C. B. Harris, N. H. Ge, R. L. Lingle, J. D. McNeill, and C. M. Wong, Annu. Rev. Phys. Chem. **48**, 711 (1997).

[7] A. Hotzel, G. Moos, K. Ishioka, M. Wolf, and G. Ertl, Appl. Phys. B **68**, 615 (1999).
[8] J. Güdde, W. Berthold, and U. Höfer, Chem. Rev. **106**, 4261 (2006).
[9] V. M. Silkin, J. Zhao, F. Guinea, E. V. Chulkov, P. M. Echenique, and H. Petek, Phys. Rev. B **80**, 121408 (2009).
[10] S. Bose, V. M. Silkin, R. Ohmann, I. Brihuega, L. Vitali, C. H. Michaelis, P. Mallet, J. Y. Veuillen, M. A. Schneider, E. V. Chulkov, P. M. Echenique, and K. Kern, New J. Phys. **12**, 023028 (2010).
[11] A. L. Vázquez de Parga, F. Calleja, B. Borca, M. C. G. Passeggi, J. J. Hinarejos, F. Guinea, and R. Miranda, Phys. Rev. Lett. **100**, 056807 (2008).
[12] B. Wang, M. L. Bocquet, S. Günther, and J. Wintterlin, Phys. Rev. Lett. **101**, 099703 (2008).
[13] B. Wang, M. L. Bocquet, S. Marchini, S. Günther, and J. Wintterlin, Phys. Chem. Chem. Phys. **10**, 3530 (2008).
[14] W. Moritz, B. Wang, M. L. Bocquet, T. Brugger, T. Greber, J. Wintterlin, and S. Günther, Phys. Rev. Lett. **104**, 136102 (2010).
[15] B. Borca, S. Barja, M. Garnica, D. Sánchez-Portal, V. M. Silkin, E. V. Chulkov, C. F. Hermanns, J. J. Hinarejos, A. L. Vázquez de Parga, A. Arnau, P. M. Echenique, and R. Miranda, Phys. Rev. Lett. **105**, 036804 (2010).
[16] H. G. Zhang, H. Hu, Y. Pan, J. H. Mao, M. Gao, H. M. Guo, S. X. Du, T. Greber, and H. J. Gao, J. Phys. Condens. Matter **22**, 302001 (2010).
[17] H. G. Zhang and T. Greber, Phys. Rev. Lett. **105**, 219701 (2010).
[18] B. Borca, S. Barja, M. Garnica, D. Sánchez-Portal, V. M. Silkin, E. V. Chulkov, C. F. Hermanns, J. J. Hinarejos, A. L. Vázquez de Parga, A. Arnau, P. M. Echenique, and R. Miranda, Phys. Rev. Lett. **105**, 219702 (2010).
[19] S. Sachs, C. H. Schwalb, M. Marks, A. Schöll, F. Reinert, E. Umbach, and U. Höfer, J. Chem. Phys. **131**, 144701 (2009).
[20] K. Donner and P. Jakob, J. Chem. Phys. **131**, 164701 (2009).
[21] T. Brugger, S. Günther, B. Wang, H. Dil, M. L. Bocquet, J. Osterwalder, J. Wintterlin, and T. Greber, Phys. Rev. B **79**, 045407 (2009).
[22] W. K. Siu and R. A. Bartynski, Phys. Rev. B **75**, 235427 (2007).
[23] See Supplemental Material at http://link.aps.org/supplemental/10.1103/PhysRevLett.108.056801 for 2PPE spectra as a function of photon energy.
[24] F. J. Himpsel, K. Christmann, P. Heimann, and D. E. Eastman, Phys. Rev. B **23**, 2548 (1981).
[25] D. Martoccia, M. Björck, C. M. Schlepütz, T. Brugger, S. A. Pauli, B. D. Patterson, T. Greber, and P. R. Willmott, New J. Phys. **12**, 043028 (2010).
[26] P. M. Echenique, R. Berndt, E. V. Chulkov, T. Fauster, A. Goldmann, and U. Höfer, Surf. Sci. Rep. **52**, 219 (2004).
[27] W. Berthold, U. Höfer, P. Feulner, and D. Menzel, Chem. Phys. **251**, 123 (2000).
[28] C. Gahl, Ph.D. thesis, Free University Berlin, 2004.
[29] D. Niesner, Th. Fauster, J. I. Dadap, N. Zaki, K. R. Knox, P.-C. Yeh, R. Bhandari, R. M. Osgood, M. Petrović, and M. Kralj, arXiv:1109.1948v1
[30] N. A. W. Holzwarth and J. R. Chelikowsky, Solid State Commun. **53**, 171 (1985).